Available online at www.sciencedirect.com
SCIENCE DIRECT
Trans. Nonferrous Met. Soc. China 16(2006) 217−222
Transactions of Nonferrous Metals Society of China
www.csu.edu.cn/ysxb/

Electro-catalytic effect of manganese oxide on oxygen reduction at teflonbonded carbon electrode

ZHOU De-bi(周德璧), LÜ Xin-kun(吕新坤), LIU Dan-ping(刘丹平)
School of Chemistry and Chemical Engineering, Central South University, Changsha 410083, China

Received 18 April 2005; accepted 8 Augest 2005

Abstract: Oxygen reduction(OR)on Teflon-bonded carbon electrodes with manganese oxide as catalyst in 6 mol/L KOH solution was investigated using AC impedance spectroscopy combined with other techniques. For OR at this electrode, the Tafel slope is –0.084 V/dec and the apparent exchange current density is $(1.02-3.0)\times10^{-7}$ A/cm^2. In the presence of manganese oxide on carbon electrode, the couple Mn^{3+}/Mn^{4+} reacts with the O_2 adsorbed on carbon sites forming O_2^- radicals and acceletes the dismutation of O_2^-, which contributes to the catalytic effect of manganese oxide for OR reaction.

Key words: oxygen reduction; manganese oxide; gas diffusion electrode; AC impedance

1 Introduction

The high performance electrocatalysts for oxygen electrode is of great importance for the development of metal-air batteries and fuel cells. As the platinum group metal based catalysts suffer from expensive cost, much work has been done to search various inexpensive electrocatalysts such as metal phthalocyanines and metal oxides. Among the electrocatalysts, manganese oxide seems to be one of the most promising candidates due to its low cost and high catalytic performance for oxygen electroreduction[1—3].

In the research of new catalysts, the basic knowledge of the mechanism of O_2 reduction and the effect of catalyst is important. Although much work has been done in this field in the last several decades, it is far from full understanding[4 — 7], due to the complexity and experimental difficulty.

Fundamental research work of oxygen reduction (OR) on porous carbon electrode is very limited. Some recent works were done on carbon electrode or on carbon electrode with platinum as catalyst, where the reported results were rather variable[8—10]. As the AC impedance method appears to be a powerful tool in studying the kinetics and mechanism of electrode reaction, it has been applied extensively in the research work on OR and on gas diffusion electrodes[11—14]. In our previous paper, we studied the OR mechanism on Teflon bonded carbon electrode in alkaline electrolyte[15]. It was found that in the OR process on gas diffusion electrode, carbon material does not act only as catalyst supporter but also provides active sites for oxygen adsorption and charge transfer. OR proceeds via a 2 electrons path where the charge transfer step producing O_2^- is followed by a superficial dismutation of these radicals to produce HO_2^- as intermediate that will be decomposed to OH^-. The materials that can accelerate the dismutation of O_2^- or HO_2^- will be good catalysts for OR in alkaline media.

The present work aims to study the mechanism and kinetics of oxygen reduction on Teflon-bonded carbon electrode with manganese oxide as catalyst. The AC impedance method was employed in combination with voltamperometric, chronopotentiometric techniques. The kinetic parameters such as exchange current density and Tafel slope were obtained and compared with those obtained on carbon supported platinum electrodes. Based on the experimental results, the mechanisms of OR and the electrocatalytic effect of manganese oxide were proposed.

Foundation item: Project(1766-394201123) supported by the Natural Science Foundation of Hunan Province, China
Correspondance author: ZHOU De-bi; Tel: +86-731-8830827; E-mail: zhoudb@mail.csu.edu.cn

2 Experimental

2.1 Electrode

The electrochemical investigation was performed on the gas diffusion electrode referred to as DE-CM in this paper, which was comprised of a single thin active layer with a nickel net as current collector. The active layer was prepared with carbon black (2.5 mg/cm^2) and manganese oxide (2.5 mg/cm^2) bonded with Teflon (2.5 mg/cm^2).

The carbon black (acetylene UV of Knapsack) has a specific surface of 50 m²/g and a density of 0.07 kg/L. The particles are in spheric form with diameters of 35—45 nm. The Mn_2O_3 powder prepared by sintering manganese carbonate at 500 °C has a specific surface (BET) of 30—50 m²/g, an average particle dimension of 30 μm and a pore diameter of 1—20 nm.

In the fabrication of the electrode, the powders of manganese oxide and activated charcoal were mixed mechanically, then the Teflon powder was added and mixed once. The mixed powders were rolled to a fine sheet with a thickness of about 0.2 mm. The sheet obtained was pressed at 100 MPa to a nickel net at room temperature, then sintered at 300 °C for 30 min.

2.2 Electrochemical cell

A two-chamber cell was used for the electrochemical measurements. The gas diffusion electrode was mounted in a Teflon holder. The geometric surface of the electrode was 1 cm². The electrolyte was 25% KOH solution prepared with the Merck extra pure grade potassium hydroxide pellets and distilled water. The reference electrode was an Hg/HgO electrode connected to the cell via a Luggin capillary. Potential values in this paper are related to the Hg/HgO electrode. The counter electrode was a platinum plate of 10 cm². The electrochemical measurements were performed at room temperature.

2.3 Electrochemical measurements

Polarization and chronopotentiometric measurements were carried out with a Model 263 EG&G Princeton potentiostat/galvanostat controlled with the M270 computer program. The polarization curves were determined in air at a scan rate of 1 mV/s, without correction for IR drop. Chronopotetiometric measurements were performed at a current of 3 μA. Impedance spectroscopy technique was also applied in our investigation. The electronic instrument consisted of an EG&G Model 5210 lock-in amplifier and the potentiostat/galvanostat. The AC frequency range was from 100 kHz to 1 mHz. The AC impedance data were collected with a M398 electrochemical program. The experimental results were analyzed with the EQUIVCRT program of Boukamp[16].

3 Results

3.1 Polarization curves

Fig.1(a) shows the linear voltammograms (LV) recorded with sweep rate of 1 mV/s at the air electrode DE-CM using Mn_2O_3 catalyst in air. For comparison, the LV curve of the air electrode prepared from carbon without Mn_2O_3 catalyst in the same condition is also given in the figure[15]. It can be seen that the rest potential is about 0.05 V on the carbon electrode in the absence of Mn_2O_3. In the presence of manganese oxide (curve DE-CM), the rest potential moves positively (0.13 V vs Hg/HgO), and the current density increases in all the potential range, showing the good catalytic effect of Mn_2O_3 for OR.

The semi-logarithmic curve ϕ vs lg[J_c/(mA·cm^{-2})] is shown in Fig.1(b) where we can see a linearity in the low overpotential range. The Tafel slope is 84 mV/dec obtained directly by regression, the apperent exchange current density is deduced as 1.02×10^{-7} A/cm^2.

Compared with that on carbon electrode without manganese oxide (J^0= 4.09×10^{-10}A/cm^2), the apparent exchange current density on DE-CM is significantly

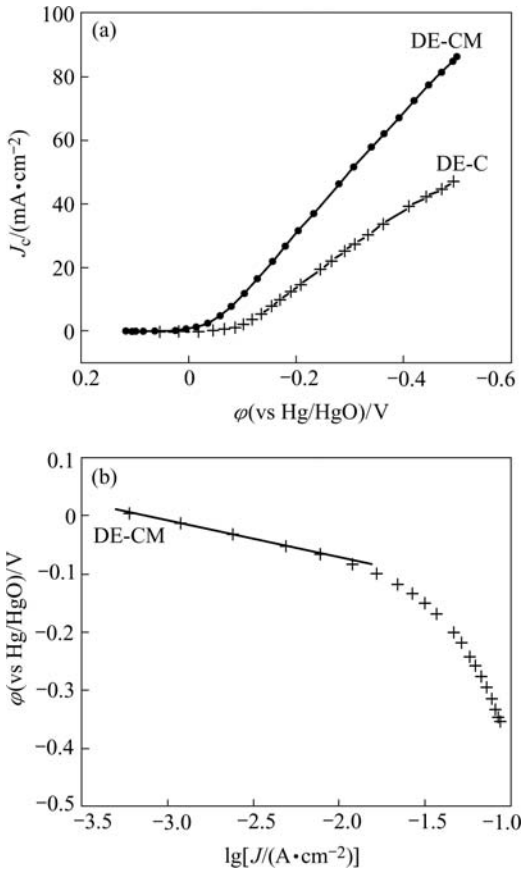

Fig.1 Polarization curves for OR on carbon electrode with Mn_2O_3 as catalyst (DE-CM)

increased. This may result from the catalytic effect of Mn_2O_3 in the charge transfer process. Meanwhile, the Tafel slope increases in the presence of Mn_2O_3, being 84 mV/dec compared with 46—84 mV/dec. This means a modification of symmetric factor a in the charge transfer process, for which we can not give a satisfactory explication.

3.2 Chronopotentiometry (CP)

The chronopotentiometric technique was applied here to measure the double-layer capacitance of electrode and the charge transfer resistance of OR near rest potential. For a relaxation procedure at low current with the effect of concentration being negligible and $R_\Omega << R_{ct}$, the overpotential can be written as

$$\eta = \varphi - \varphi_{eq} = IR_{ct}(1 - e^{-t/\tau}) \quad (1)$$

where φ is the potential at current I and $\tau = C_{dl}R_{ct}$. For $t \to \infty$, $\eta_\infty = IR_{ct}$, the charge transfer resistance R_{ct} is thus obtained and we have the following relationship:

$$\ln\left(1 - \frac{\eta}{\eta_\infty}\right) = -\frac{t}{\tau} \quad (2)$$

By tracing the $\ln(1-\eta/\eta_\infty)$ plot, we can obtain the relaxation time constant and hence the double-layer capacity C_{dl}. The principle of this technique was described in our previous paper[15].

In our measurements, the applied current was 15 μA. The chronopotentiograms recorded is shown in Fig.2(a). It can be seen that with the small cathodic current applied, the electrode's overpotential increases with time and reaches a stable value after 450 s. The $\ln(1-\eta/\eta_\infty)-t$ plot shows a good linearity. The kinetic parameters obtained from the CP measurement are given in Table 1.

3.3 Impedance spectroscopy

The impedance diagrams for OR at −0.2 V and −0.4 V on DE-CM are shown in Fig.3 and Fig.4 respectively. The Nyquist plots at two potentials show similar features. We can see two capacitive loops in the applied frequency range from 10 kHz to 10 mHz. The Bode plot shows more evidently the turn point at frequency of 1 Hz that separates the two capacitive arcs.

3.4 Data fitting

Although the equivalent circuit approach is looked down upon by some, analyzing EIS data by fitting it to equivalent circuit models can be a valid and rewarding approach. To fit the experimental data, we have proposed several circuits, the best fitting results were obtained with the circuit $R_\Omega(C_{dl}[R_{ct}O])(R_cW)$ as shown in Fig.5. The element R_Ω is the serial ohmic resistance

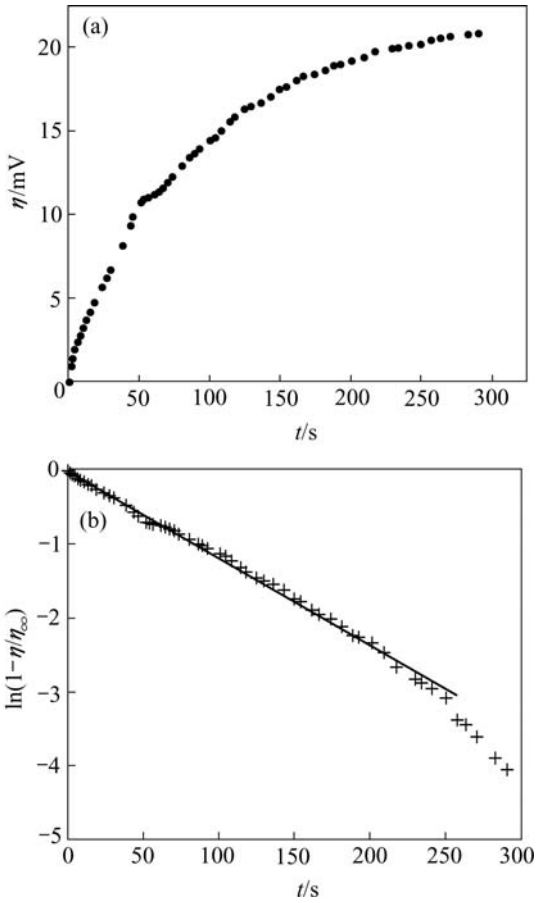

Fig.2 Chronopotentiograms on electrode DE-CM in 6 mol/L KOH solution at 20 ℃ (I =0.015 mA)

Table 1 Kinetic parameters for OR DE-CM by CP and ac impedance measurements

Parameter	DE-CM			DE-C		
	Rest	−0.2 V	−0.4 V	Rest	−0.2 V	−0.40 V
$R_\Omega/(\Omega\cdot cm^2)$		1.15	1. 13		0.98	1.27
$C_{dl}/(mF\cdot cm^{-2})$	6.49	15.1	14.5	25.3	16.9	34.1
$R_{ct}/(\Omega\cdot cm^2)$	1.4×10^3	1.31	0.78	6.7×10^3	0.80	13.0
$\sigma_O/(\Omega\cdot S^{-1/2})$		4.72	5.05		19.7	8.40
$\delta D^{-1/2}/s^{1/2}$		0.71	0.62		1.26	1.30
$R_C/(\Omega\cdot cm^2)$		1.35	2.11		4.23	8.57
$\sigma_W/(\Omega\cdot S^{-1/2})$		37.1	37.8		17.5	10.8

* The parameters for OR at rest potential were obtained by CP measurements; the others at –0.2 and –0.4V (vs Hg/HgO) by EIS.

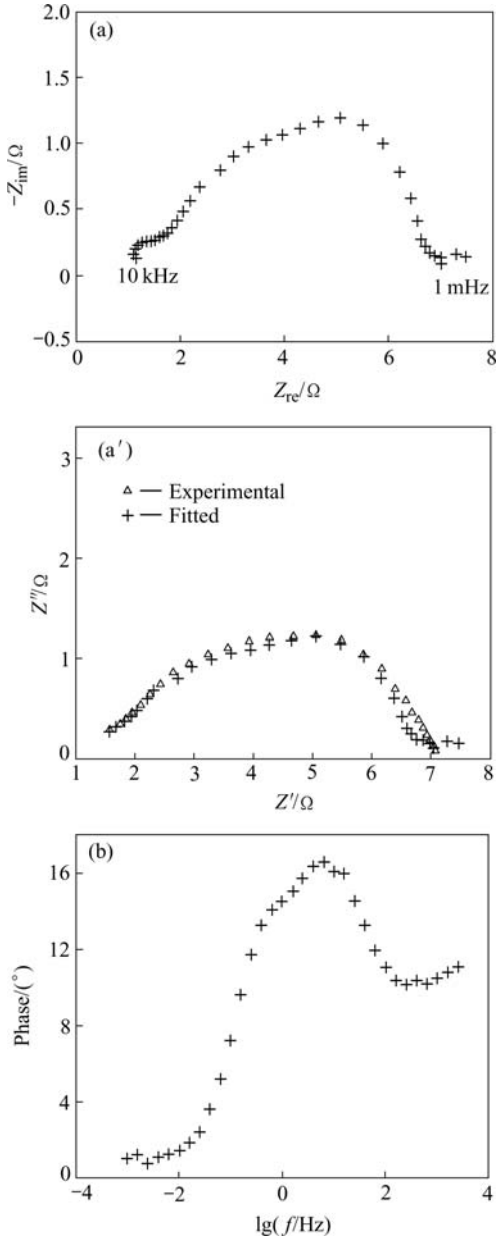

Fig.3 Impedance diagrams recorded on carbon electrode at −0.2 V (vs Hg/HgO) in 6 mol/L KOH: (a) Nyquist plots (experimental and fitted); (b) Bode plot

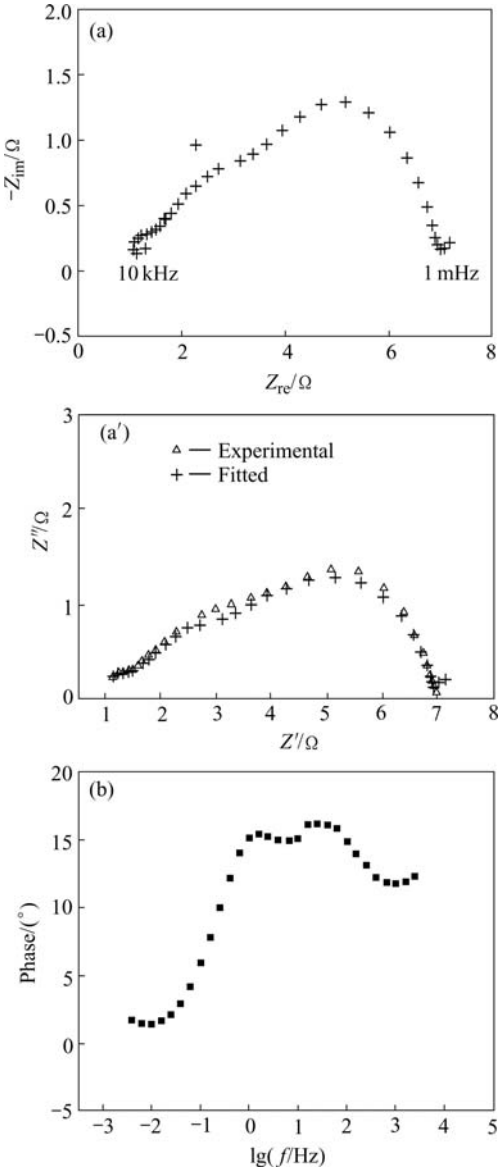

Fig.4 Impedance diagrams recorded on carbon electrode at −0.4 V (vs Hg/HgO) in 6 mol/L KOH: (a) Nyquist plots (experimental and fitted); (b) Bode plot

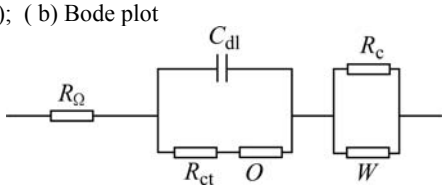

Fig.5 Equivalent circuit for fitting impedance spectra

of electrode and electrolyte. The parallel circuit (C_{dl}[$R_{ct}O$]) corresponds to the electrode/electrolyte interfacial reaction with C_{dl} for the double-layer capacitance, R_{ct} for the charge transfer resistance and O for the thin-layer diffusion impedance. The parallel circuit (R_cW) composed of a resistance and a Warburg diffusion impedance is not quite easy to understand. To interpret this feature, we suggest that as a step of OR reaction, the charge transfer process is followed by two parallel paths: 1) a diffusion of the product of the charge transfer process ; 2) a chemical reaction which does not proceed in the double-layer (without a capacitive behavior) but is potential dependent. The resistance R_c may be attributed to the chemical reaction.

For OR at −0.2 V, the circuit $R_\Omega(C_{dl}[R_{ct}O])(R_cW)$ and $R_\Omega(C_{dl}[R_{ct}O])(R_cO)$ gave fitting results without much difference. For the data at −0.4 V, when the circuit $R_\Omega(C_{dl}[R_{ct}O])(R_cW)$ was applied, some parameters were not quite consistent with these at −0.2 V. We tried the circuit $R_\Omega(C_{dl}[R_{ct}O])(R_cO)$ where the O (Nernst Layer Diffusion) was used instead of W and got better fitting results. The parameters obtained are given in Table 1.

Comparing the parameters obtained at different

potentials, we notice that as the potential of electrode gets more negative (from rest potential to −0.4 V), the charge transfer resistance R_{ct} decreases. Meanwhile, the double-layer capacitance increases as potential changes from rest potential to −0.2 V, which may be due to a better wettability of electrode surface at −0.2 V and −0.4 V. The parameters obtained with the two different techniques (CP and EIS) are quite consistent.

The values of the parameters at −0.2 V and −0.4 V are very approaching, implying that there is not significant difference in the reaction mechanism and in the mass transport condition at these different potentials.

To understand the catalytic effect of Mn_2O_3 for OR, we compared in the same table the parameters obtained on DE-CM and on DE-C, the latter is the carbon electrode in the absence of manganese oxide[15].

As revealed by the equivalent circuit, the OR on the carbon electrode may consist of a charge transfer process in serial with a chemical reaction with the parameters R_{ct} and R_c representing their reaction rates respectively. We can see from Table 1 that for the carbon electrode without catalyst (DE-C), R_c is much larger than R_{ct}; while for DE-CM, R_c decreases significantly and the total resistance (R_{ct}+R_c) is much decreased at all potentials, which shows the good catalytic effect of Mn_2O_3 in the charge transfer process and more significantly in the following chemical reaction.

Compared with that on carbon electrode DE-C, the values of C_{dl} of DE-CM decreases, which may be due to the lower specific surface and wettability of Mn_2O_3 than those of carbon black. We notice also that the Nernst diffusion process is improved at DE-CM, which can be attributed to the modification of electrode structure by replacing part of carbon black with Mn_2O_3.

4 Discussion

4.1 Pathway of oxygen reduction on Mn_2O_3 catalytic carbon electrode

In our study of OR on carbon electrode in the absence and presence of Mn_2O_3 catalyst, the AC impedance feature is characterized by a circuit (R_cW) in addition to the interfacial faradaic reaction. To interpret this feature, we recall our previous study of OR on platinum electrode[13] where we supposed the following mechanism for OR at weak overpotential:

$$O_2+e^- \xrightarrow{i} O_{2,ad}^-$$

$$2O_{2,ad}^- + H_2O \xrightarrow{r} O_2 + HO_2^- + OH^-$$

$$HO_2^- + H_2O \rightleftharpoons H_2O_2 + OH^-$$

Based on this mechanism, we deduced a simplified equivalent circuit including a circuit ($R_\theta C_\theta$) for the chemical reaction.

OR on carbon electrode can be interpreted by this mechanism and the (R_cW) has similarity to ($R_\theta C_\theta$). According to the mechanism, OR is an E-cat-C (Electro-Catalyze-Chemical) type reaction. The radical superoxide $O_{2,ad}^-$ forms in the electron transfer step and adsorbs on the electrode. HO_2^- formed can be reduced at electrode in the following steps or diffuse into electrolyte. This mechanism favors the 2 e path leading to the formation of H_2O_2.

Based on the above fact, we propose that at carbon electrode even catalyzed by Mn_2O_3, oxygen reduction proceeds through peroxide pathway where the molecular oxygen is reduced to HO_2^-, followed by further reduction of HO_2^- or its direct decomposition to OH^-.

The catalytic activity of manganese oxides for the decomposition of H_2O_2 is well known[17]. KANUNGO et al proposed that the decomposition of hydrogen peroxide is based on the simultaneous oxidation and reduction of the surface manganese ions, which suggests that the catalytic activity is closely related with the electrochemical activity. In our present investigation, we have found the catalytic effect of Mn_2O_3 on OR, which may be mainly attributed to its effect on the decomposition of HO_2^- and H_2O_2.

Mechanism of catalytic effect of Mn_2O_3 on charge transfer process at carbon electrode

We can see from the experimental results of this study that, the resistances of the charge transfer reaction and the following chemical reaction for OR on carbon electrode decreases significantly in the presence of Mn_2O_3, which means the effect of manganese oxide in these steps.

The effect of association of carbon black and Mn_2O_3 on OR activity can be explained by the stabilization of the couple Mn^{3+}/Mn^{4+} on carbon surface. The oxygen chemically adsorbed on carbon is transferred in OR and frees the C sites. We can consider that a mixed equilibrium between Mn_2O_3/MnO_2 and C/CO_{ads} assures the transfer of oxygen from atmosphere to formation of electroactive adsorbed oxygen.

We try to interprete the catalytic effect of manganese oxide on OR. The first action involved in aqueous electrolyte is the hydroxylation of Mn_2O_3:

$$Mn_2O_3 + H_2O \Leftrightarrow 2MnOOH$$

In the presence of carbon, the couple Mn^{3+}/Mn^{4+} exists on the Mn_2O_3 surface and brings in the following reaction:

$$2MnOOH + 1/2\,O_2 \Leftrightarrow 2MnO_2 + H_2O$$

At room temperature and under high oxygen partial pressure, the equilibrium will shift toward right.

In the presence of carbon, the reaction will proceed toward left due to the affinity of carbon to oxygen as carbon provides much active sites for oxygen adsorption.

The reaction schema can be proposed as

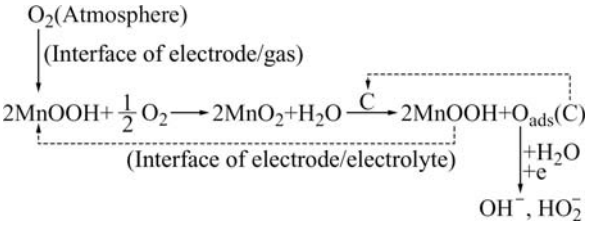

where the MnOOH/MnO_2 and C/C(O) systems function as electro-catalytic couple.

For the effect of the couple Mn_2O_3/C on the dismutation reaction, we may present the following manner:

$$C-O_2^- + H_2O + Mn^{3+} \rightarrow C + HO_2^- + OH^- + Mn^{4+}$$

$$C-O_2^- + Mn^{4+} \rightarrow C + O_2 + Mn^{3+}$$

The dismutation reaction is hence accelerated through two parallel reactions instead of a slow reaction between two negative radicals. The catalytic action of manganese oxide on H_2O_2 dismutation is well known .

In the high alkaline electrolyte without O_2 between −0.3 V and −0.5 V (vs Hg/HgO), Mn_2O_3 transforms to Mn_3O_4 and MnO. At potentials more negative than −0.4 V, Mn_2O_3 will lose its catalytic effect. In the electrode DE-CM prepared with same mass of carbon and Mn_2O_3, the volume of carbon is larger, so that the Mn_2O_3 particles are dispersed in carbon. During the sintering with Teflon, carbon black protects Mn_2O_3 particles from excessive oxidation.

5 Conclusions

1) For oxygen reduction at the electrode with manganese oxide as catalyst in 6 mol/L KOH solution, the Tafel slope is −0.084 V/dec (vs Hg/HgO) and the exchange current density is $(1.02-3.0)\times10^{-7}$ A/cm^2 that increases by 2 order of magnitude compared with that on carbon electrode without catalyst.

2) At carbon electrode even catalyzed by Mn_2O_3, oxygen reduction proceeds through the peroxide pathway where the molecular oxygen is reduced to HO_2^-, followed by further electrochemical reduction or chemical disproportionation reaction of HO_2^- to OH^-.

3) In the presence of manganese oxide on carbon electrode, the couple Mn^{3+}/Mn^{4+} reacts with the O_2 adsorbed on carbon sites forming O_2^- radicals and accelerates the dismutation of O_2^-, which contributes to the catalytic effect of manganese oxide for OR reaction.

References

[1] CAO Y L, YANG H X, AI X P, XIAO L F. The mechanism of oxygen reduction on MnO_2-catalyzed air cathode in alkaline solution[J]. Journal of Electroanalytical Chemistry, 2003, 557: 127−134.

[2] BŘETISLAV KLÁPŠTĚ, JIŘÍ VONDRÁK, JANA VELICKÁ. MnO_x/C composites as electrode materials(II): Reduction of oxygen on bifunctional catalysts based on manganese oxides[J]. Electrochimica Acta, 2002, 47: 2365−2369.

[3] YANG J, XU J J. Nanoporous amorphous manganese oxide as electrocatalyst for oxygen reduction in alkaline solutions[J]. Electrochemistry Communications, 2003, 5: 306−311.

[4] BOCRIS J O'M, ABDU R. A theoretical study of the electrochemical reduction of oxygen[J]. J Electroanal Chem, 1998, 448: 189−204.

[5] ZHOU D B, VANDER POORTEN H. Impedance characteristics of oxygen reduction at platinum electrode in alkaline electrolyte[J]. J Electrochem Soc, 1998, 145: 936.

[6] YEAGER E. Electrocatalysts for O_2 reduction[J]. Electrochim Acta, 1984, 29: 1527−1537.

[7] DAMJANOVIC A, BRUSIC V. Electrode kinetis of oxygen reduction on oxide-free platinum electrodes[J]. Electrochem Acta, 1967, 12: 615−628 .

[8] KENJO T, KAWATSU K. Current-limiting factors and the location of the reaction area in PTFE-bended double-layered oxygen electrodes[J]. Electrochim Acta, 1985, 30: 229.

[9] HOLZE R, VIELSTICH W. The kinetics of oxygen reductions at porous Teflon-bonded fuel cell electrodes[J]. J Electrochem Soc, 1984, 131: 2298 .

[10] STRIEBEL K A, MCLARNON F R, CAIRNS E J. Fuel cell cathode studies in aqueous K_2CO_3 and KOH[J]. J Electrochem Soc, 1990, 137: 3360.

[11] ARICÒ A S, ALDERUCCI V, ANTONUCCI V, FERRARA S, RECUPERO V, GIORDANO N, KINOSHITA K. AC impendance spectroscopy of porous gas diffusion electrode in sulphunic acid[J]. Electrochim Acta, 1992, 37: 523−529.

[12] SELMAN J R, LIN Y P. Application of ac impendance in fuel cell research and developmeng[J]. Electrochim Acta, 1993, 38: 2063−2073.

[13] ZHOU D B, VAMDER POORTEN H. Electroconductive membrane 'Celec' for pplication in Zinc/Air alkaline batteries—An impedance study of oxygen reduction at the interface Pt/ 'Celec' [J]. J Appl Electrochem, 1996, 26: 833−841.

[14] ØSTERGARD M J L, MOGENSEN M. AC impedance study of the oxygen reduction mechanism on $La_{1-x}Sr_xMnO_3$ in solid oxide fuel cells[J]. Electrochim Acta, 1993, 38: 2015−2020 .

[15] ZHOU De-bi, HUANG Ke-long, ZHANG Si-min. Oxygen reduction on Teflon-bonded carbon electrode[J]. Trans Nonferrous Met Soc China, 2004, 14(4): 817−823.

[16] BOUKAMP B A. Users Manual of Equivalent Circuit[M]. The Netherlands: Twente University, 1989.

[17] MAO Lan-qun, ZHANG Dun, SOTOMURA T, NAKATSU K, KOSHIBA N, OHSAKA T. Mechanistic study of the reduction of oxygen in air electrode with manganese oxides as electrocatalysts[J]. Electrochimica Acta, 2003, 48: 1015−1021.

(Edited by YUAN Sai-qian)